

# An Infrared study of the Josephson vortex state in high- $T_c$ cuprates

S.V. Dordevic<sup>1</sup>, Seiki Komiya<sup>2</sup>, Yoichi Ando<sup>2</sup>, Y.J. Wang<sup>3</sup>, and D.N. Basov<sup>1</sup>

<sup>1</sup> *Department of Physics, University of California, San Diego, La Jolla, CA 92093*

<sup>2</sup> *Central Research Institute of Electric Power Industry, Tokyo, Japan*

<sup>3</sup> *National High Magnetic Field Laboratory, Tallahassee, FL 32310*

We report the results of the c-axis infrared spectroscopy of  $\text{La}_{2-x}\text{Sr}_x\text{CuO}_4$  in high magnetic field oriented parallel to the  $\text{CuO}_2$  planes. A significant suppression of the superfluid density with magnetic field  $\rho_s(H)$  is observed for both underdoped ( $x=0.125$ ) and overdoped ( $x=0.17$ ) samples. We show that the existing theoretical models of the Josephson vortex state fail to consistently describe the observed effects and discuss possible reasons for the discrepancies.

Although the mechanism of high- $T_c$  superconductivity in cuprates still remains unresolved, significant progress has been made in understanding of the mixed state of these systems [1]. Many subtle predictions of the theories of the vortex state have been experimentally verified [1–17]. In particular, electrodynamics in relatively small magnetic fields (typically  $H < 7$  T) appears to be in accord with the models proposed for both pancake vortices formed with  $\mathbf{H} \perp \text{CuO}_2$ -planes, and for the Josephson vortices developing in the  $\mathbf{H} \parallel \text{CuO}_2$ -plane configuration [2–7]. In this work we explored field-induced suppression of the superfluid density in  $\text{La}_{2-x}\text{Sr}_x\text{CuO}_4$  (LSCO) single crystals due to Josephson vortices. By extending previous studies to stronger fields (up to 17 T) we find marked departures of the experimental data from conventional Josephson vortex theory. In particular the superfluid density in underdoped LSCO appears to be much more fragile than the models prescribe. The implications of these findings for our current understanding of cuprates will be discussed.

We used infrared (IR) spectroscopy to examine the interlayer ( $\mathbf{E} \parallel c$ ) response of high quality LSCO crystals [18]: an underdoped with  $x=0.125$  ( $T_c \simeq 32$  K) and a weakly overdoped with  $x=0.17$  ( $T_c \simeq 36$  K). The near-normal-incidence reflectance  $R(\omega)$  was collected over a broad temperature (6–300 K) and frequency (10–48,000  $\text{cm}^{-1}$ ) range. In addition field-induced changes of the reflectivity  $R(H, 6\text{K})/R(0\text{T}, 6\text{K})$  were measured under zero field cooling with  $\mathbf{H} \parallel \text{CuO}_2$ , when vortices penetrate in-between the  $\text{CuO}_2$  planes [15]. The uncertainty of the absolute measurements in our apparatus does not exceed 0.5 %, whereas the relative errors of the field-induced changes are less than 1 %. The optical conductivity  $\sigma_1(\omega) + i\sigma_2(\omega)$  and the dielectric function  $\epsilon_1(\omega) + i\epsilon_2(\omega)$  were calculated from  $R(\omega)$  using Kramers-Kronig analysis.

In the superconducting state the real part of the optical conductivity has two components:  $\sigma_1^{SC}(\omega) = \frac{\rho_s}{8}\delta(0) + \sigma_1^{reg}(\omega)$ , the first one due to superconducting condensate and the second due to unpaired carriers below  $T_c$  (a so called regular contribution). The superfluid density  $\rho_s$  is quantified with the plasma frequency  $\omega_s$ :  $\rho_s = \omega_s^2 = c^2/\lambda_c^2 = 4\pi e^2 n_s/m^*$  related to the density of superconducting carriers  $n_s$  and their mass  $m^*$ ;  $\lambda_c$  is the

penetration depth. A delta function in  $\sigma_1^{SC}(\omega)$  gives rise to a term  $-(\omega_s/\omega)^2$  in  $\epsilon_1(\omega)$ . A common procedure of extracting  $\omega_s$  from  $\epsilon_1(\omega)$  involves fitting of the low energy part of the spectrum with  $1/\omega^2$ . The problem with this procedure is that it does not discriminate screening due to superconducting condensate from regular contribution. In order to fix this problem we use the following correction procedure:

$$\epsilon_1(\omega) - \epsilon_1^{reg}(\omega) = -\frac{\omega_s^2}{\omega^2}, \quad (1)$$

where  $\epsilon_1^{reg}(\omega)$  is the regular contribution to dielectric function. In order to calculate  $\epsilon_1^{reg}(\omega)$  a KK-like transformation is employed:

$$\epsilon_1^{reg}(\omega) = 1 + \frac{2}{\pi} \int_0^\infty \frac{\omega' \epsilon_2^{reg}(\omega')}{\omega'^2 - \omega^2} d\omega', \quad (2)$$

where  $\epsilon_2^{reg}(\omega)$  is the regular contribution to the imaginary part of dielectric constant, i.e. after a  $\delta(0)$ -function has been subtracted. The procedure described by Eq. 1 and 2 accounts for contribution of unpaired carriers at  $T < T_c$ , but also phonons, interband transitions, magnons, and all other finite energy excitations.

Figure 1 displays the raw reflectance data. In zero field the 6 K reflectance of both LSCO crystals is characterized by a sharp plasma edge at the frequency  $\omega_s/\sqrt{\epsilon_\infty}$  ( $\epsilon_\infty$  is the high frequency dielectric constant). This form of reflectance, which resembles a plasma edge in normal metals, is due to the zero crossing in the real part of the dielectric function,  $\epsilon_1(\omega) = 0$ , and is commonly referred to as the Josephson Plasma Resonance (JPR). As temperature increases, the edge in  $R(\omega)$  is smeared out and the minimum shifts to lower frequency, indicating suppression of the superfluid density. In the normal state the underdoped sample shows a very weak upturn of  $R(\omega)$  as  $\omega \rightarrow 0$ , indicating a small metallic contribution at  $T > T_c$ . The upturn is stronger in the  $x=0.17$  crystal suggesting that the far IR conductivity increases with doping. Similar enhancement of the "metallic" trends in the interlayer response is commonly found in other cuprate families.

Application of a magnetic field has a strong impact on the JPR feature in both crystals (bottom panels): the

plasma edges are smeared and the minima in  $R(\omega, H)$  also shift to lower  $\omega$ . The plasma edge shift in 17 T field is as strong as 35 % in the  $x=0.125$  sample and 10 % in the  $x=0.17$  crystal. This result is surprising given the fact that the strongest field used in our experiments is still orders of magnitude smaller than the upper critical field  $H_{c2}$  for the  $\mathbf{H} \parallel \text{CuO}_2$  orientation.

It is instructive to present the evolution of the superconducting condensate with  $H$  and  $T$  with the spectra of the loss function  $Im(1/\epsilon(\omega)) = \epsilon_2(\omega)/(\epsilon_1^2(\omega) + \epsilon_2^2(\omega))$  (Fig. 2). At  $T \ll T_c$  the loss function is peaked at the frequency close to the JPR, whereas the width of the  $Im(1/\epsilon(\omega))$  mode is proportional to the magnitude of  $\epsilon_2(\omega, T < T_c)$ . As temperature increases the peak shifts to lower energies, indicating suppression of the superfluid density. The insets in the top panels show the temperature dependence of the superfluid density closely resembling the form expected for a  $d$ -wave superconductor. At the lowest measured temperature we found the following values of the superfluid density:  $\omega_s=160 \text{ cm}^{-1}$  ( $\lambda_c = 9.7 \mu\text{m}$ ) for 12.5 % sample and  $\omega_s=360 \text{ cm}^{-1}$  ( $\lambda_c = 4.3 \mu\text{m}$ ) for 17 % material.

The behavior of the loss function in high magnetic field (Fig. 2 bottom panels) is generally similar to the  $H=0$  data taken at finite temperature: the peak softens and its width is enhanced as the field increases. Fig. 3A quantifies the demise of  $\omega_s$  in magnetic field. At 17 T the superfluid density is reduced by 38 % in the underdoped and 12 % in the overdoped sample; these values are in full agreement with the strength of the effect inferred directly from raw data in Fig. 1. We also note qualitatively different form of the  $\omega_s(H)$  dependencies in the two samples. Two principal mechanisms of the superfluid density suppression in high magnetic field are: 1) direct pair-braking of the condensate and 2) dissipation associated with vortex dynamics. The former process is usually discarded in view of giant  $H_{c2}$  values in the  $\mathbf{H} \parallel \text{CuO}_2$  configuration. Within the latter picture the oscillating electric field with the  $\mathbf{E}$ -vector along the  $c$ -axis leads to a transverse motion  $u$  of Josephson vortices [1] located between the  $\text{CuO}_2$  planes in the direction perpendicular to the field (see the bottom inset of Fig. 2). Electrodynamics of Josephson vortices has been thoroughly discussed in several papers. [14–16] Below we show that the behavior of JPR in LSCO crystals cannot be fully understood within the proposed models, especially in the underdoped sample.

Bulaevskii *et al* have worked out the following prediction for the field dependence of  $\omega_s$ : [16]

$$\omega_s(H) = \omega_0 \left[ 1 - \frac{\pi}{8} \frac{H}{H_0} \ln \frac{H_0}{H} \right]. \quad (3)$$

The effect of magnetic field is directly related to the strength of the coupling between the  $\text{CuO}_2$  layers that is parameterized through the characteristic field  $H_0 = \Phi_0/\gamma s^2$ . In this expression  $\Phi_0$  is the flux quantum,

$\gamma = \lambda_c/\lambda_{ab}$  ( $\lambda_{ab}$  is the in-plane penetration depth) is the anisotropy factor and  $s \simeq 1.32 \text{ nm}$  is the interlayer distance. We estimated  $H_0=36.7 \text{ T}$  for the  $x=0.125$  with  $\lambda_{ab} = 0.2 \mu\text{m}$  (Ref. [19]) and  $H_0 = 55 \text{ T}$  for the  $x=0.17$  sample with  $\lambda_{ab} = 0.3 \mu\text{m}$  (Ref. [19]). In Fig. 3B we plot  $\omega_s(H)/\omega_s(0)$  as a function of  $H/H_0$  along with the theoretical dependence (full line). The overall trends of  $\omega_s(H)$  are clearly different for the two crystals. In particular, the  $x=0.125$  material reveals a dramatic reduction of the condensate strength compared to the model prediction for  $H/H_0 > 0.3$ . For  $x=0.17$  sample such high magnetic fields could not be achieved with the present experimental setup.

We also attempted to describe  $\omega_s(H)$  within a phenomenological scenario of vortex dynamics [14,15]. Tachiki, Koyama and Takahashi (TKT) [15] obtained an explicit result for the complex dielectric function of a layered superconductor in the mixed state:

$$\epsilon(\omega) = \epsilon_\infty - \frac{\frac{\omega_n^2}{\omega^2 + i\gamma_{sr}\omega} + \frac{\omega_s^2}{\omega^2}}{1 + \frac{\phi_0}{4\pi\lambda_c^2} \frac{H}{\kappa_p - i\eta\omega - M\omega^2}}, \quad (4)$$

where  $M$  is the vortex inertial mass,  $\eta$  is the viscous force coefficient and  $\kappa_p$  is the vortex pinning constant. In Eq. 4,  $\epsilon_\infty$  is the real part of the dielectric function above the plasmon and  $\omega_n$  and  $\gamma_{sr}$  are the regular component (due to unpaired carriers below  $T_c$ ) plasma frequency and scattering rate. Eq. 4 can be regarded as a  $H \neq 0$  generalization of the well known "two fluid" model of superconductivity, commonly used in the microwave and IR frequency ranges [21]. In order to model the data in Fig. 3 we extracted the  $\omega_s(H)$  behavior from Eq. 4 by exploring  $\text{Re}[\epsilon(\omega)]$  in the limit of  $\omega \rightarrow 0$ :  $\omega_s^2 = \omega^2 \times \epsilon_1(\omega)$ . Some of the parameters of the TKT equation needed to obtain this result were readily available from the fits of  $R(\omega, 6K, H = 0)$ :  $\epsilon_\infty=27$ ,  $\omega_n=200 \text{ cm}^{-1}$  (for 12.5 % sample) and  $1,100 \text{ cm}^{-1}$  (for 17 % sample),  $\gamma_{sr}=5,000 \text{ cm}^{-1}$ . Similar to all previous spectroscopic works [5,6,22] we set the vortex mass to zero in Eq. 4. The viscous drag constant  $\eta$  can be calculated within Coffey-Clem approach [14] yielding  $\eta=7 \text{ Pa cm}$  and  $28 \text{ Pa cm}$ , for the underdoped and overdoped samples respectively. [23] Therefore we are left with the pinning force constant  $\kappa_p$  as the only fitting parameter in Eq. 4. As Fig. 3A shows the theory gives a very good fit for the overdoped sample, with  $\kappa_p = 6,000\text{--}11,000 \text{ Pa}$ , a value comparable with that of nearly optimally doped  $\text{YBa}_2\text{Cu}_3\text{O}_y$  [22] (in the same field configuration). For the underdoped sample on the other hand, we could not obtain a good fit for any value of  $\kappa_p$ . In order to reproduce the overall depression of the superfluid density in 17 T field we have to adopt  $\kappa_p=150\text{--}200 \text{ Pa}$ . We believe that such a vast difference in the magnitude of  $\kappa_p$  between the two samples is another signal of inability of the TKT scenario to account for the experimental situation at least in underdoped LSCO crystals.

One obvious distinction between the underdoped and overdoped samples is the different nature of the inter-layer transport. Earlier experiments [24] established that the  $x=0.16$  doping in the LSCO system separates the region of "insulating" (for  $x<0.16$ ) and "metallic" ( $x>0.16$ ) ground states. This result may have important implications for the nature of the  $\mathbf{H} \parallel \text{CuO}_2$ -vortices. The  $x=0.125$  crystal is likely to fall in the regime where a description within the formalism of Josephson vortices is applicable owing to the insulating character of the "medium" separating the  $\text{CuO}_2$  planes. However, as doping progresses to the over-doped side eventually the  $\mathbf{H} \parallel \text{CuO}_2$ -vortices will evolve into Abrikosov-type vortices having a normal core. Therefore our  $x=0.17$  crystal may be closer to the regime where additional factors involving complex character of the vortex cores in  $d$ -wave superconductors have to be taken into consideration. [13,25,26] Surprisingly, the Josephson analysis (Eqs. 3 - 4) obviously ignoring the latter issues, is less problematic for the  $x=0.17$  crystal but fails for the  $x=0.125$  sample which, based on its "insulating" resistivity at  $T \rightarrow 0$ , is likelier to comply with Eqs. 3 - 4. In particular, the TKT analysis yields an unexpectedly small pinning constant which is hard to reconcile with prominence of the intrinsic inhomogeneities in underdoped cuprates, since inhomogeneities would normally promote vortex pinning.

When searching for reasons for the inability of Eqs. 3 - 4 to consistently describe the anomalous sensitivity of the superfluid response in underdoped LSCO to magnetic field it is prudent to revisit the assumptions of these models. Indeed, Eqs. 3 - 4 are valid for Josephson coupling between *uniform*  $s$ -wave superconductors; validity of both assumptions for high- $T_c$  materials is questionable. One implication of the  $d$ -wave order parameter (firmly established for cuprates) is that the Zeeman energy associated with the  $\mathbf{H} \parallel \text{CuO}_2$  field can no longer be disregarded for states close to the node. [27] The impact of the Zeeman field is especially important for the  $x=0.125$  phase since at this particular composition the magnitude of the in-plane superconducting gap is anomalously low. [28] The field-dependence of the  $c$ -axis superfluid density within this scenario has the following form:  $\omega_s^2(H)/\omega_s^2(0) = \sqrt{1 - (H/\Delta)^2}$  [29] and is displayed in Fig.3C for different magnitudes of the energy gap  $2\Delta$ . Interestingly, the functional form of  $\omega_s(H)/\omega_s(H=0)$  is reproduced by this calculation. The Zeeman reduction of the condensate strength occurs in concert with other dissipation mechanisms and accounts for at least 10-15% depression of the  $\omega_s(17T)$  value. An additional factor pertinent to the anomalous field response of the underdoped crystals may be connected to spatial non-uniformities of superconductivity *within* the  $\text{CuO}_2$  planes revealed by a variety of experimental methods. [30]. It seems plausible that the magnetic field will influence coupling between these dissimilar regions in the  $\text{CuO}_2$  plane thus leading to field-dependence of the *in-plane* superconducting pa-

rameters such as  $\lambda_{ab}$  in Eq. 3.

Models of the superfluid density suppression discussed above involve only a reduction of carrier density  $n_s$ . However, the  $c$ -axis response of cuprates also reveals changes of the effective mass  $m^*$  or of the kinetic energy at  $T < T_c$ . [31] Recently Ioffe and Millis proposed that the variation the effective mass below  $T_c$  is connected with phase coherence between the  $\text{CuO}_2$  planes. [32] Phase coherence is suppressed in magnetic field which may lead to a more rapid degradation of the superfluid density via the increase of  $m^*$  in addition to usual reduction of  $n_s$ . This latter effect is expected to be particularly strong in underdoped samples which show the strongest changes of  $m^*$  at  $T < T_c$ . [31]

In conclusion, magneto-optical results for underdoped LSCO revealed remarkable depression of the superfluid density in the vortex state. We have identified several factors which may account for much more complex behavior of underdoped LSCO beyond conventional Josephson vortex models. Further theoretical analysis is needed to distinguish between the roles played by spatial non-uniformities of superconducting state, as well as by changes of kinetic energy in the observed behavior. In this fashion quantitative understanding of vortex state data presented in this work will be instrumental in narrowing down the range of plausible theoretical descriptions of the underdoped state cuprates.

We thank D.P. Arovas, L. Bulaevskii, Ch. Helm, J.R. Clem, M. Coffey, A.E. Koshelev, T. Koyama and A.J. Millis for useful discussions. The research supported by NSF, DoE, the Research Corporation and the State of Florida.

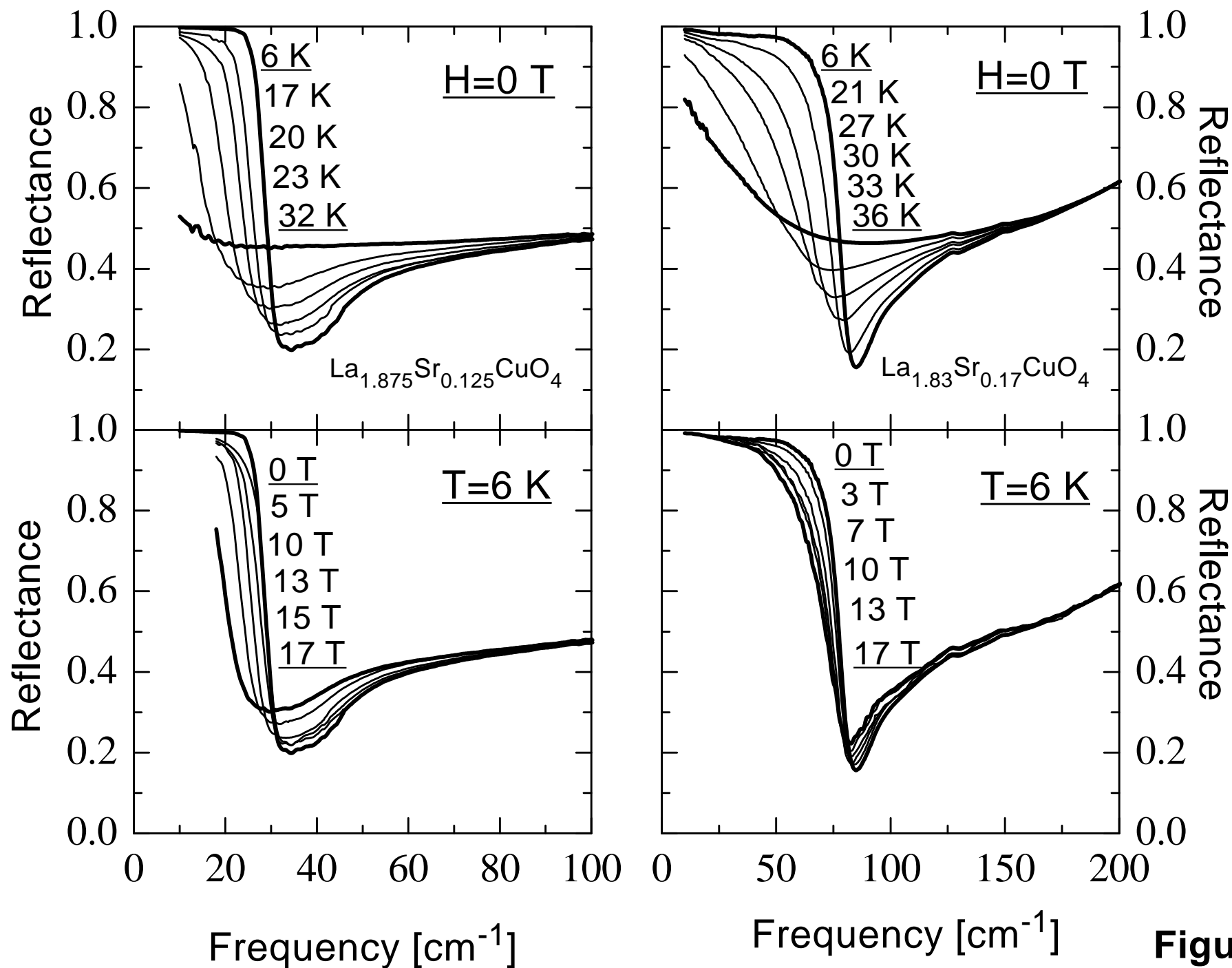
- 
- [1] Blatter G., *et al.*, *Rev.Mod.Phys.* **66** (1994) 1125.
  - [2] Yeh N.-C., *Phys.Rev.B* **43** (1991) 523.
  - [3] Feinberg D., *et al.*, *Phys.Rev.Lett.* **65** (1990) 919.
  - [4] Doyle R.A., *et al.*, *Phys.Rev.Lett.* **71** (1993) 4241.
  - [5] Parks B., *et al.*, *Phys.Rev.Lett.* **74** (1995) 3265.
  - [6] Gerrits A.M., *et al.*, *Phys.Rev.B* **51** (1995) 12049.
  - [7] Dulic D., *et al.*, *Phys.Rev.Lett.* **86** (2001) 4660.
  - [8] Pimenov A., *et al.*, *Phys.Rev.Lett.* **87** (2001) 177003.
  - [9] Pesetski A.A., *et al.* *Phys.Rev.B* **62** (2000) 11826.
  - [10] Choi E.-J., *et al.*, *Phys.Rev.B* **49** (1994) 13271.
  - [11] Koshelev A.E., *et al.*, *Phys.Rev.Lett.* **81** (1998) 902.
  - [12] Matsuda Y., *et al.*, *Phys.Rev.Lett.* **75** (1995) 4512.
  - [13] Lake B., *et al.*, *Science* **291** (2001) 1759.
  - [14] Coffey M.W., *et al.*, *Phys.Rev.Lett.* **67** (1991) 386.
  - [15] Tachiki M., *et al.*, *Phys.Rev.B* **50** (1994) 7065.
  - [16] Bulaevskii L.N., *et al.*, *Phys.Rev.Lett.* **74** (1995) 801.
  - [17] Lihn H.-T.S., *et al.*, *Phys.Rev.B* **56** (1997) 5559 (1997).
  - [18] Ando Y., *et al.*, *Phys.Rev.Lett.* **87** (2001) 017001.
  - [19] Uchida S., *et al.*, *Phys.Rev.B* **53** (1996) 14558.
  - [20] Kim J.H., *et al.*, *Physica C* **247** (1995) 297.

- [21] Hosseini A., *et al.*, *Phys.Rev.B*, **60** (1999) 1349.
- [22] Wu D.H., *et al.*, *Phys.Rev.Lett.* **65** (1990) 2074.
- [23] These values are much smaller than typical values measured previously for the vortex motion *across* the planes [33], in qualitative agreement with a theoretical prediction [34]  $\eta_{\parallel}/\eta_{\perp} \approx \lambda_c^2/3\lambda_{ab}^2 \sim 1,000 - 3,000$ . In the configuration studied here (see the bottom inset of Fig. 2) because of "intrinsic pinning" [4] one intuitively expects viscous effects (i.e. dissipation) to be much smaller than for the vortex motion across the planes.
- [24] Boebinger G.S., *et al.*, *Phys.Rev.Lett.* **77** (1996) 5417.
- [25] Arovas D.P., *et al.*, *Phys.Rev.Lett.* **79** (1997) 2871.
- [26] Han J.H., *et al.*, *Phys.Rev.Lett.* **85** (2000) 1100.
- [27] Yang K. and Sondhi S.L., *Phys.Rev.B* **57** (1998) 8566.
- [28] Dumm M., *et al.*, *Phys.Rev.Lett.* **88** (2002) 147003. IR measurements of the in-plane response of the x=0.125 LSCO crystal show that the superfluid density is collected from the frequency range below 70-80  $\text{cm}^{-1}$ . This sets up the upper bound for the magnitude of  $2\Delta(0)$  whereas the analysis of the  $\omega$ -dependence suggests that gap value can be as small as 40  $\text{cm}^{-1}$ .
- [29] Won H., *et al.*, *Physica B* **281-282** (2000) 944.
- [30] Wakimoto S., *et al.*, *Phys.Rev.B* **62** (2000) 3547; Hoffman J.E., *et al.*, *Science* **295** (2002) 466; Lang K.M., *et al.*, *Nature* **415** (2002) 412.
- [31] Basov D.N., *et al.*, *Science* **283** (1999) 49.
- [32] Ioffe L.B. and Millis A.J., *Science* **285** (1999) 1241.
- [33] Golosovsky M., *et al.*, *Phys.Rev.B* **50** (1994) 470.
- [34] Hao Z., *et al.*, *IEEE Trans.Magn.* **27** (1991) 1086.

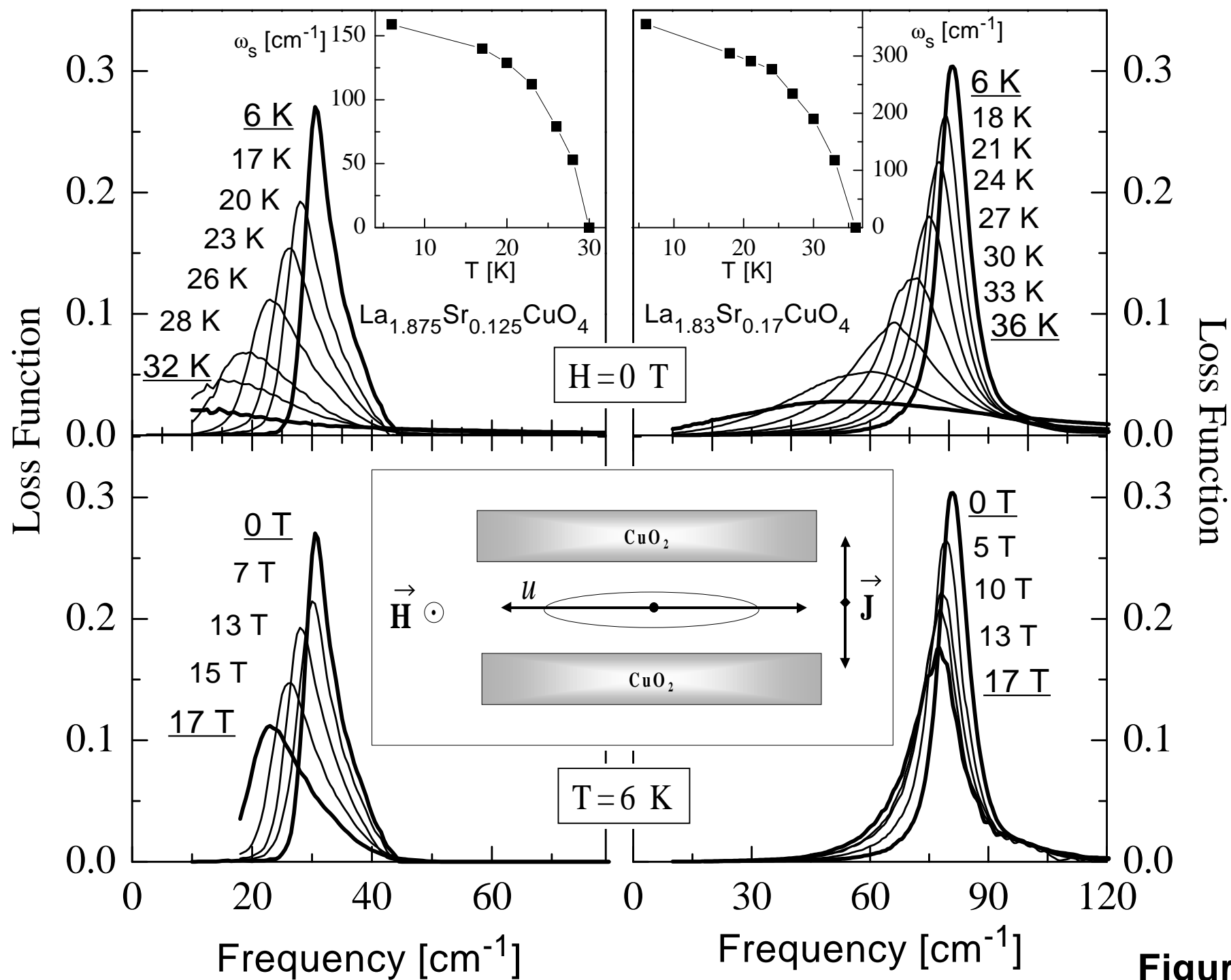
FIG. 1. Infrared data for LSCO crystals with x=0.125 (left panels) and x=0.17 (right panels). The top panels show c-axis reflectance in zero field; the bottom panels:  $R(\omega)$  in high magnetic field.

FIG. 2. The loss function  $\text{Im}(1/\epsilon(\omega))$  reveals coupling to the longitudinal JPR mode. The top two panels show the temperature dependence of the loss function and the bottom ones the loss function in high magnetic field. The top insets show the temperature dependence of the superfluid density and the bottom one sketch the geometry of a Josephson vortex experiment.

FIG. 3. Change of the superfluid density with magnetic field  $\omega_s(H)/\omega_s(0)$  alone with the theoretical results obtained for the TKT model (panel A), Bulaevskii *et al* model (panel B) and scenario taking into account the nodal Zeeman effect (panel C). While conventional models of the Josephson vortex state are inconsistent with the high field data for the underdoped x=0.125 crystal (A and B), plausible description can be achieved within the picture discussed by Won *et al.* [29] using the magnitude of the gap in from the in-plane measurements for the same crystal [28].



**Figure 1**



**Figure 2**

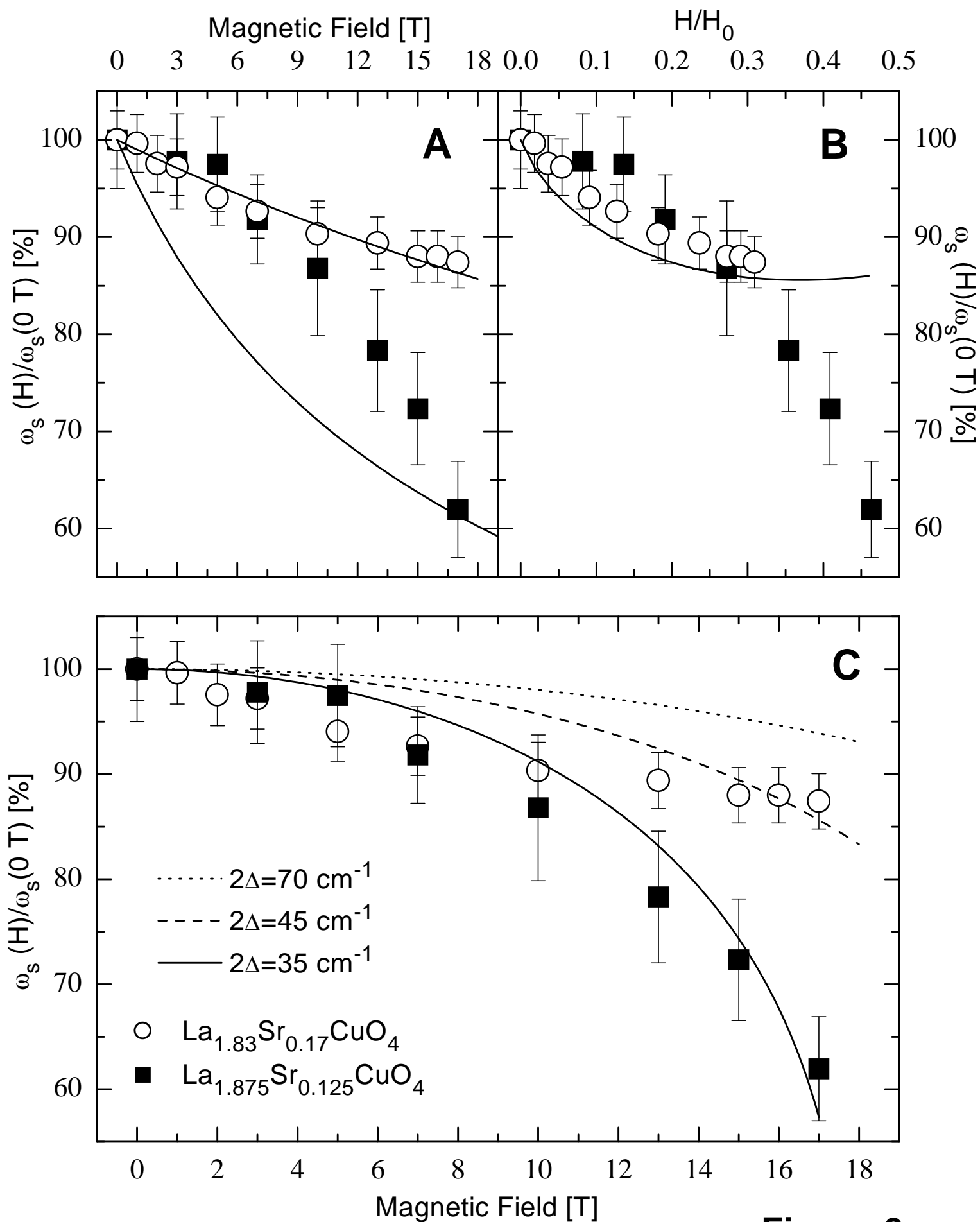


**Figure 3**